IEEE Access
Multidisciplinary | Rapid Review | Open Access Journal

Received February 26, 2022, accepted March 10, 2022, date of publication March 14, 2022, date of current version March 25, 2022.

Digital Object Identifier 10.1109/ACCESS.2022.3159687

Analysis of Tension Instability and Research on Stability Control Strategy in the Process of Rapier Loom Weaving

YANJUN XIAO[1,2,3], FURONG HAN[1,3], WEILING LIU[1], FENG WAN[1], AND KAI PENG[1]

[1]School of Mechanical Engineering, Hebei University of Technology, Tianjin 300130, China
[2]Tianjin Key Laboratory of Power Transmission and Safety Technology, Department of State Key Laboratory Reliability and Intellectual Electrical, Tianjin 300130, China
[3]Career Leader Intelligent Control Automation Company, Suqian, Jiangsu 223800, China

Corresponding authors: Yanjun Xiao (xyj@hebut.edu.cn) and Weiling Liu (h282325471@163.com)

This work was supported in part by the Science and Technology Plan Project of Jiangsu Province under Grant BRA2020244.

ABSTRACT Tension control is very important for the intelligent control system of rapier looms because stable tension guarantees a tight fabric structure, moderate elasticity and good forming. To solve the problems of low-tension measurement accuracy of the existing rapier loom, the complex structure of the tension control strategy and algorithm, and the high research and development cost, this paper proposes new research from the perspective of high-precision and nonlinear processing of tension detection signals. The median filtering and limiting filtering algorithms are integrated to solve the uncertainty problem caused by the disturbance and fluctuation of the tension signal, and an excellent sample dataset is obtained. The attenuation factor and the number of learning times are introduced to design and adjust the learning rate of the back propagation neural network algorithm. In addition, the overfitting problem of the backpropagation neural network model in the current research process is solved. The experimental simulation results show that the tension detection fluctuation range of this method is 0.8 kg, and the tension detection error is within 0.1%. On the basis of the existing tension control algorithm, the tension detection accuracy is improved, which presents a new research perspective for the wide application of high-precision tension control strategies in rapier looms. It is of great importance to improve the production efficiency and fabric quality of rapier looms.

INDEX TERMS Algorithm fusion, backpropagation neural network, digital filtering, rapier loom, tension detection, tension control.

I. INTRODUCTION

Rapier looms have many advantages, such as high speed, high automation, high-efficiency production and strong adaptability of manufacturing varieties. It is currently an essential piece of production equipment in the textile industry. However, due to the complex structure of the warp let-off mechanism of the rapier loom, the warp tension tends to fluctuate greatly during the weaving process, which causes the warp to break or the fabric structure to loosen, thereby affecting the quality of the fabric. Stable tension guarantees a tight fabric structure, moderate elasticity and good forming. Therefore, research on tension control strategies for rapier looms is of great importance for improving the quality and level of fabric manufacturing of rapier looms [1]–[4].

The associate editor coordinating the review of this manuscript and approving it for publication was R. K. Tripathy.

At present, the research work is mainly focused on the two aspects of the intelligent tension control algorithm and improving the tension detection level to obtain accurate control of loom tension. Liu et al [5] established a dynamic model of warp tension through dynamic analysis of a carbon fiber multilayer skew weaving machine and designed an adaptive fuzzy PID controller. Compared with PID control, the output tension fluctuation is small, and it has a better control effect. Xu *et al.* [6] analyzed the force of the warping and coiling mechanism of a carbon fiber multilayer oblique weaving machine, established a mathematical model of tension control, constructed a loom tension control strategy based on the equivalent sliding mode control and Lyapunov theory, and demonstrated the stability of the system. Lin *et al.* [7] proposed a particle-based smoothed particle hydrodynamics (SPH) interface force detection algorithm. The stability and accuracy of the algorithm to

simulate the interface force are verified by an example. Liu *et al.* [5], [8] proposed a single neuron adaptive control strategy based on a quadratic performance index. The optimal control method is used to minimize the sum of the square of the output error and the control increment to adjust the parameters of the controller. Karnoub *et al.* [10] established a simulation model suitable for warp tension calculation and used a genetic algorithm and gradient algorithm to optimize the parameters of the loom. The simulation results show that the use of the optimized loom settings can eliminate fabric defects. Xu *et al.* [11] shot a light source on yarn and analyzed the relationship between the image size of the yarn diameter on the CCD and the change in tension to detect the tension of the yarn. Banitalebi *et al.* [12] used eddy current technology to realize the dynamic measurement of the yarn.

Through a literature review, it is apparent that an improvement of the tension detection has mainly been approached from the perspectives of optical detection, smooth particle hydrodynamic interface force detection, and the selection of smart sensors. These research methods have high environmental requirements when applied to tension detection and are not suitable for rapier looms under complex working conditions [13]–[16]. The intelligent tension control algorithm of the loom has given new vitality to the traditional algorithm. Research on loom tension control based on intelligent algorithms, such as fuzzy control, equivalent sliding mode control, and genetic algorithms has made rich progress, and the tension control accuracy has been improved. However, the above intelligent optimization control algorithms all have the following two shortcomings:

(1) In the process of optimizing the tension control algorithm, only the control tension is considered to ensure that the tension is kept stable. The optimized processing of the tension signal is not considered, which makes the error of the signal itself larger and affects the further improvement of the tension control accuracy.

(2) There are many parameters that need to be adjusted, the calculations of the algorithm are numerous, and the structure is complex, which results in high research and development costs for the system, and thus, cannot be widely used for universal loom equipment. The development limitations are relatively large.

Therefore, it is urgent to design a new tension control algorithm. This algorithm needs to optimize the tension signal, reduce the error of the tension signal, and improve the tension control accuracy. In addition, it is necessary to reduce the algorithm structure, reduce the amount of calculation, and reduce the cost of research and development to ensure that it can be applied to universal loom equipment.

An ANN has the ability to find optimal solutions at a high speed. A feedback artificial neural network designed for a certain problem can quickly find an optimized solution and is expected to solve the problem of a complex algorithm structure. As a powerful tool for optimizing processing parameters, it is widely used in various research fields [17], [18]. Ylma *et al.* [19] used the DE/rand/1 mutation strategy to train a Pi-sigma artificial neural network through a differential evolution algorithm. The performance of the proposed method is evaluated on two datasets, and was found that the proposed method has very effective performance compared with many artificial neural network models. Yildirim *et al.* [20] proposed a threshold single multiplication neuron artificial neural network training algorithm based on the harmony search algorithm and particle swarm optimization and evaluated the performance of the proposed method through simulation studies. Lin *et al.* [21], [22] established a deep belief network (DBN) model to predict the true stress of superalloys based on experimental data. The results showed that the established DBN model had good predictability for the high-temperature deformation behavior of the studied alloy.

The above research shows that the fusion of artificial neural network algorithms and related intelligent algorithms or systems can accurately and quickly process multiple complex parameters at the same time, and the data processing accuracy obtained can exceed 99%.

Therefore, combined with the characteristics of the original tension signal, the tension control accuracy of rapier looms is further improved while reducing the training time and research and development costs. This paper proposes a new tension control strategy for rapier looms based on the fusion of a back propagation (BP) neural network and a digital filter algorithm. In the process of this tension control strategy, an excellent dataset is obtained by fusing the median-filter algorithm and the limiting-filter algorithm. Then, the BP neural network algorithm is introduced for high-precision data fitting [23]–[29]. The simulation results show that without changing the existing hardware structure or increasing the development costs, the detection range of the selected tension sensor is 850 kg, the tension detection fluctuation range of this algorithm is 0.8 kg, and the tension detection error is within 0.1%. Improvement of the tension control precision of rapier looms is of great importance for improving the production efficiency and quality of the fabric [30]–[35].

The main innovations and contributions of this article are as follows:

(1) The BP neural network algorithm is optimized. The attenuation factor and number of learning times are introduced to the design to adjust the learning rate of the BP neural network algorithm. Based on the nonlinear model of rapier loom tension detection and control, as well as on the principle of neural network parameter setting, a novel learning rate calculation model is proposed. The problem of ''overfitting'' or the slow convergence time of the network that may be caused by the unreasonable setting of the learning rate in the current research process is solved, and the accuracy and speed of the tension control strategy are improved. In addition, the theoretical system of the BP neural network is improved by optimizing the algorithm of the BP neural network.

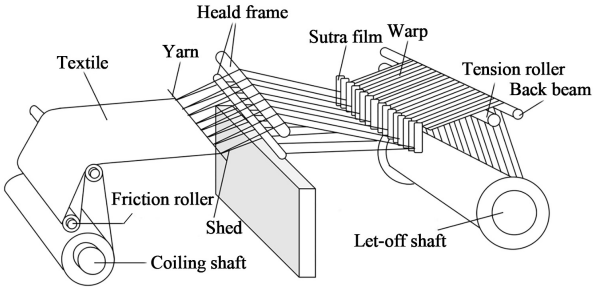

FIGURE 1. The mechanical structure of a rapier loom.

(2) A new research perspective is proposed considering the high precision and nonlinearity of the tension detection signal. This furthers the existing research that only considered the control tension level, which caused the processed signal to have a relatively large error, and thus, required an improvement of the tension control accuracy. It fills the gap in the existing research on the optimization of the tension detection signal and enriches the research content on the tension control of rapier looms.

(3) A new tension control strategy for rapier looms is proposed. The proposed tension control strategy is composed of a digital-filter algorithm fused with a median-filter algorithm and a limiting-filter algorithm and an optimized BP neural network. In the digital-filter algorithm, the median-filter and the limiting-filter algorithms are combined to process the tension detection signal. The fluctuation range of the tension detection signal is reduced, and an excellent sample dataset can be obtained. The BP neural network algorithm partly analyzes the nonlinear relationship between the input and the output through the learning and prediction capabilities of the neural network to obtain optimized data processing results. The tension control strategy has a simple algorithm structure and a small amount of calculation. It greatly reduces the research and development costs of the system and provides a theoretical basis for the popular application of high-precision rapier loom tension control strategies in universal loom equipment.

II. PRINCIPLE OF TENSION DETECTION FOR RAPIER LOOMS

The mechanical structure of a rapier loom is complex. In the weaving process, all parts need to cooperate to complete the fabric production. The warp yarn is wound on the let-off shaft, supported by the tension roller and the fixed back beam, and separated into individual yarns through the stop piece. Then, the heald frame completes the opening action in the up and down directions. The opening shuttles are shuttled back and forth by the loom shuttle carrying the weft yarn to complete the weaving process. Then, the finished fabric is wound onto the take-up shaft through the mechanism of the friction roller. The mechanical structure of a rapier loom is shown in Fig. 1.

When weaving, the warp on the let-off shaft bypasses the fixed back beam, and the finished fabric is wound on the take-up shaft through the action of the intermediate

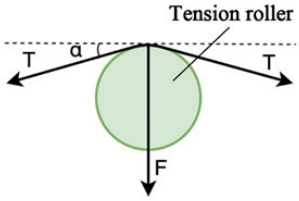

FIGURE 2. Schematic diagram of the warp tension force transfer model.

structure. In this process, the warp continues to produce a consistently changing force on the tension roller. Therefore, the mechanical structures directly related to loom tension detection are the tension roller and the fixed back beam. Fig. 2 shows a schematic diagram of the warp tension force transfer model, where T is the warp tension and F is the pressure exerted by the warp on the tension roller.

The mathematical expression of the warp tension T is as follows:

$$F = 2T\sin\alpha \tag{1}$$

F is the conversion of warp tension into pressure on the tension roller and α is the initial tension angle of the warp. Through the tension force transmission model, the warp pressure received by the tension roller can be detected to detect the warp tension. First, the warp tension is transferred to the elastic body through the setting of the mechanical structure and converted into the strain of the elastic body. Then, the resistance strain effect is used to obtain its strain value. The tension value of the warp yarn is detected indirectly.

The tension control of the loom is one of the important factors to ensure the stable and reliable operation of the loom, and effective tension detection is a necessary condition for tension control. The complex mechanical structure of the loom, the weaving process and the harsh production environment all have an impact on the tension signal. Under the influence of the abovementioned factors, the collected tension signal shows the law that the fluctuation range of the tension value is random and the change range is uncertain.

III. DIGITAL FILTERING ALGORITHM FUSION

The original tension signal has the characteristics of a relatively slow change process. The tension value fluctuates randomly, and the variation amplitude is uncertain. It has the characteristics of a sharp increase in value changes and large jumps, and the range of signal amplitude changes between two adjacent sampling results are uncontrollable. The two signal characteristics show a sequential relationship in the signal processing procedure that presents a fusion relationship in constraints. The median-filter algorithm is more effective for pulsation interference caused by fluctuations, which is caused by accidental factors in the slow-changing process or errors due to the sampling instability. It is suitable for removing the fluctuation caused by accidental factors or the pulsation interference caused by the instability of the sampler. However, it takes a certain amount of time to change many physical quantities during the production process. Therefore, the range of change between two adjacent

sampled values should be within a certain limit. The median-filter algorithm cannot limit the large range of amplitude changes caused by random interference or distortion caused by the instability of the sampler. As a result, tension signal processing cannot achieve the expected effect. To resolve this shortcoming, this paper proposes a novel digital filtering algorithm that combines a median filtering algorithm and a limiting filtering algorithm. The original tension signal is processed to solve the contradiction that the original signal features present a fusion relationship in the constraints. It also reduces the fluctuation range of the tension detection sampling information and obtains a relatively pure tension detection signal with small errors, as well as achieves an effective signal anti-interference processing effect.

A. RESEARCH ON THE DIGITAL FILTER FUSION ALGORITHM

The internal logic of the median-filter algorithm is to sort first and then select the median value as the final value. The inherent logic of the limiting-filter algorithm is to use the limiting principle to determine the input signal and reduce all instantaneous values that exceed the preset threshold too close to the previously set threshold.

First, N continuous samplings of the tension information parameters are performed, and N is generally an odd number. Then, the appropriate threshold value A is determined based on experience or the maximum deviation allowed during two samplings. Then, the two sampled values at adjacent moments are compared. If the difference between the two sampled values is greater than the maximum deviation threshold A, then random interference or surge interference is considered. The last sampled value is regarded as an illegal value, and the delete operation is given. After deletion, the previous sampling value is used to replace the next sampling value. If the difference does not exceed the maximum allowable deviation threshold A, the sampled value is considered valid and adopted. Finally, the processed values of the N samplings are arranged in ascending order, and the intermediate value is selected as the final value of the sampling. In this paper, by combining the limiting-filter algorithm with the median-filter algorithm, the amplitude of the original tension signal fluctuation is greatly reduced. In addition, the sampling fluctuation amplitude is limited, which solves the obvious fluctuation problem of the original tension signal. The program design flow chart of the digital fusion algorithm is shown in Fig. 3.

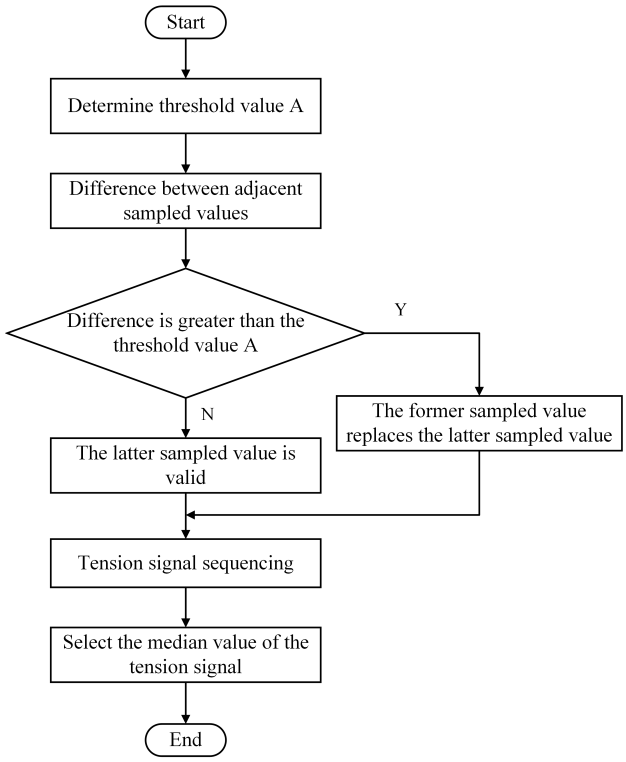

FIGURE 3. Digital filter fusion algorithm program design flow chart.

IV. BP NEURAL NETWORK DATA FITTING

A. DATA FITTING

After the tension sampling data is processed by digital filtering, relatively clean and usable data can be obtained. However, the desired results cannot be obtained directly from this data. The loom tension detection system needs to detect the loom tension in real-time, and obtain the specific tension value through the reverse conversion of the mathematical equation. The matching process of the input and output requires data fitting and cooperation. The data fitting method is the least square method, which is commonly used in the tension detection field. Nevertheless, because of the error interference in practical applications, the relationship between the input and the output is not strictly linear. Therefore, this paper also employs the learnability and the predictability of the neural network method to compensate for the defects of the least squares method, analyze the nonlinear relationship between the input and the output, obtain better results and realize the substitution of the algorithm.

B. WORKING PROCESS OF THE BP NEURAL NETWORK

When the BP neural network is working, it is necessary to determine the topological structure of the neural network and initialize the relevant parameters after the data is input. Then, the information enters into the real training work, the actual output is obtained through calculation, and whether or not the error meets the relevant conditions is determined. If it is satisfied, the output is output; if it is not satisfied, the weight threshold needs to be adjusted and updated by error backpropagation. Through many training and learning steps, the objective function value is more in line with the requirements to obtain the final BP neural network and solve the related problems.

C. THEORETICAL DERIVATION OF BP NEURAL NETWORK DATA FITTING

The structure of a BP neural network generally consists of three layers: an input layer, a hidden layer and an output

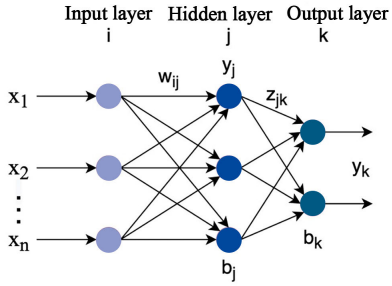

FIGURE 4. Schematic diagram of the BP neural network theoretical model.

layer. The input layer and the output layer are single-layer structures, whereas the hidden layer can be a multilayer structure, and each layer can be composed of single or multiple neuron nodes. Each layer of the three-layer network structure is distributed with a certain number of nodes. There is no connection short message between the nodes in the layer, but the adjacent nodes are connected through the relevant weights to form the whole network. The theoretical model of the BP neural network is shown in Fig. 4.

In Figure 4, i=1,2…n, j=1,2…n. $x_i$represents the i-th input variable, and w_{ij} represents the weight of the i-th input variable, which is linked to the j-th hidden layer node. y_j represents the output result of the j-th hidden layer node and it is also the input variable of the output layer node. z_{jk} represents the relative weight of the output result of the jth hidden layer linked to the node of the kth output layer. b_j represents the threshold of the jth hidden layer node, and b_k represents the threshold of the kth output layer node. y_k represents the final output result of the k-th output layer node.

The working process of the BP neural network is divided into two processes: the forward transmission process of input information and the backpropagation process of error information.

(1) Forward transmission of input information

The forward transmission process of input information refers to the process where the information enters the network from the input layer, and it is transmitted to the output layer after the relevant processing of the hidden layer.

We let the node activation function of the hidden layer be f (v); then, the output result of the j-th node of the hidden layer is as follows:

$$y_j = f\left(\sum_{i=1}^{p} w_{ij}x_i + b_j\right), (j = 1, 2 \ldots p) \tag{2}$$

w_{ij} represents the weight of the i-th input variable, which is linked to the j-th hidden layer node; x_i represents the i-th input variable; and b_j represents the threshold on the j-th output layer node.

We let g (v) be the node activation function of the output layer; then, the output result of the k-th node of the output layer is as follows:

$$y_k = g\left(\sum_{j=1}^{s} z_{jk}y_j + b_k\right), (k = 1, 2 \ldots s) \tag{3}$$

z_{jk} represents the correlation weight of the jth hidden layer output result linked to the kth output layer node; b_k represents the threshold value on the kth output layer node; and y_j represents the final output result of the kth output layer node.

(2) Backpropagation process of error information

The total error of the whole network is calculated as follows:

$$E\,(w, b) = \frac{1}{2}\sum\nolimits_{k=1}^{s} e_k^2 \tag{4}$$

where e_k represents the node error of the output layer.

The correction of the whole backpropagation process is divided into the adjustment of weights and thresholds from the output layer to the hidden layer and from the hidden layer to the input layer.

① Weight and threshold correction from the output layer to the hidden layer

First, the weight z_{jk} needs to be corrected. The direction of correction should be the inverse gradient of $E - z_{jk}$, which is the direction with the fastest decline. We let η be the learning rate of the neural network. Then we can obtain the equation as follows:

$$\Delta z_{jk}\,(n) = -\eta\frac{\partial E\,(n)}{\partial z_{jk}(n)} \tag{5}$$

n represents the nth variable of the input.

② Weight and threshold correction from the hidden layer to the input layer

Similar to the weight correction from the output layer to the hidden layer, the weight correction $\Delta w_{ij}(n)$ from the hidden layer to the input layer is as follows:

$$\Delta w_{ij}\,(n) = -\eta\frac{\partial E\,(n)}{\partial w_{ij}\,(n)} \tag{6}$$

D. BP NEURAL NETWORK DATA FITTING ALGORITHM OPTIMIZATION AND MODEL CONSTRUCTION

(1) Establishment of the model and network structure

Assuming that the model structure is a nonlinear model, the calculation is as follows:

$$y = X^T + \sum_{j}^{M} c_j \max\left(0, X^T\theta_j\right) \tag{7}$$

In Formula (7), the unknown parameters of the model include hyperparameter M, parameter $\theta_j(0 \leq j \leq M)$, and parameter $c_j(0 \leq j \leq M)$.

We suppose the connection weight and bias terms are $w_i(i = 1, 2)$ and $b_i(i = 1, 2)$, and the output of the i-th neuron in the hidden layer is $h_i^n(n = 1; 0 \leq i \leq M)$. The BP neural network algorithm designed by this system uses 3 layers. The input matrix is expressed as $X = [X_1, X_2]$. The model needs to augment the input matrix X, and then multiply it by the

parameter $\theta_j(0 \leq j \leq M)$, which is equivalent to the bias term in the neural network.

(2) Determination of the activation function

The activation function of the neural network in this system selects the ReLU function, $f(x) = \max(0,x)$. The purpose of this is to remove the linearization of the entire neural network output and make the entire neural network model nonlinear.

(3) Setting the loss function and forward propagation algorithm

The loss function selected in the algorithm is the mean square error (MSE) function, which uses the mean square error and the derivative of the activation function to update the weights and biases. The specific formula is as follows:

$$E(y, \bar{y}) = \frac{\sum_{i=1}^{n} (y - \bar{y})^2}{n} \tag{8}$$

Assuming that for the i-th neuron in the n-th layer, there are M (M is a hyperparameter) neurons in the n-1 layer that are connected to the neuron by synapses, then the input of the i-th neuron in the n-th layer is as follows:

$$Layer_I^n = \sum_{j=1}^{M} w_j^n h_j^{n=1} + b_j^n \tag{9}$$

The output of the ith neuron in the nth layer is as follows:

$$h_j^n = Max\left(Layer_I^n\right) \tag{10}$$

(4) Setting the backpropagation algorithm

Combining Formula (9) and Formula (10), we can obtain the relationship between the input of the i-th neuron in the nth layer and the output of the i-th neuron in the n-1 layer as follows:

$$Layer_I^n = \sum_{j=1}^{M} w_j^n Max\left(Layer_I^n\right) + b_j^n \tag{11}$$

According to the mean square loss function in Equation (8), the weight gradient and bias term gradient of the jth neuron in the nth layer can be obtained by mathematical induction as follows:

$$\begin{cases} \frac{\partial E(i)}{\partial W_{ji}^{(l)}} = \delta_j^{(l)} h_i^{(l-1)} \\ \frac{\partial E(i)}{\partial b_j^{(l)}} = \delta_j^{(l)} \end{cases} \tag{12}$$

(5) Setting the gradient descent algorithm

After obtaining the gradient of the connection weight and the bias term of each hidden layer, the learning rate and the gradient descent algorithm are used to update the connection weight and the bias term of each layer as follows:

$$\begin{cases} W_{ji}^{(l)} = W_{ji}^{(l)} + learn_{rate} \times \frac{\partial E(i)}{\partial W_{ji}^{(l)}} \\ b_j^{(l)} = b_j^{(l)} + learn_{rate} \times \frac{\partial E(i)}{\partial b_j^{(l)}} \end{cases} \tag{13}$$

In Formula (13), $2 \leq \| \leq L - 1$.

(6) BP neural network algorithm optimization: designing an update strategy for learning rate improvement.

This step is the most critical in this model design process and directly affects the accuracy and the speed of tension signal processing. Since the learning rate of the BP neural network is fixed, if the learning rate is set too large, it leads to overfitting of the model; if it is set too small, the convergence speed of the network becomes slow. Therefore, the optimal learning rate is not a fixed value, but it should change as the number of training iterations decays. This article introduces the attenuation factor and the number of learning times to achieve real-time adjustment of the learning rate. Based on the nonlinear model constructed in step (1) and the principle of a neural network parameter setting, a new calculation model for scores can be developed to slow the learning rate as follows:

$$learn\_\_rate = \frac{learn_{rate}}{1 + step * decay} \tag{14}$$

First, we set the initial learning rate and start from 0.001. Then, the magnitude is changed to 0.01. The convergence speed of the neural network can be observed and a more appropriate initial learning rate is determined. Then, the decay factor is slowly adjusted in real-time to control the slowdown of the learning rate and maintains it within a reasonable range.

The working conditions, environment and products of rapier looms are similar. After the system is adjusted and stabilized, the relevant conditions are relatively stable, meaning that the working conditions do not change. Therefore, this method is consistent with the rapier loom system.

(7) Normalization and anti-normalization

In the neural network model, the output of each neuron cannot be negative. Therefore, it is necessary to normalize the data and substitute the initial data when denormalizing. In this way, the positive and negative characteristics of the initial data can be transferred to the predicted data, thereby predicting the negative value. In addition, normalization is used to unify calculation standards.

(8) Setting a random restart algorithm

To prevent a local minimum when updating parameters, a random restart method is used to replace the initial parameter state.

(9) Determination of hyperparameter M

Hyperparameter M of this program is determined using a random search method, and the value of M is determined to be 20.

BP neural network algorithm implementation process: First, the parameters of the neural network, such as the number of network layers, the input and output nodes, the threshold, the bias, the number of iterations, and the termination conditions are initialized. Then, the training samples are input, and the output and error of each layer are calculated via the related formulas. Next, the weights of each layer are adjusted according to the error. Finally, it is

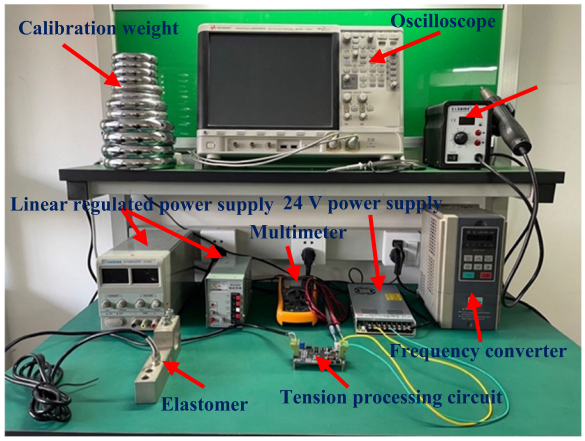

FIGURE 5. Laboratory experiment platform.

determined whether or not the termination condition is met, the output is created, and if the training is continued.

V. EXPERIMENTAL TEST

The experimental test in this paper is divided into two stages, namely, the laboratory environment test and the field production environment test. The two complement each other and combine to form a complete test platform for the tension detection system of the loom.

A. LABORATORY ENVIRONMENTAL TESTING

As shown in Fig. 5, the experimental platform in the laboratory environment is composed of calibration weights, oscilloscopes, hot air guns, linear stabilized power supplies, multimeters, 24 V power supplies, frequency converters, elastomers, and tension processing circuits. It can meet the requirements of the frequency converter interference test, the power supply test, the tension signal acquisition test and the tension signal processing test in the laboratory environment.

1) DIGITAL FILTERING ALGORITHM FUSION EXPERIMENT

We collect 1000 sets of data under 10 kg of tension for an experiment, determine that the median filter window size is 7 and set the maximum threshold value to 150. We test the effect and feasibility of the fusion of the median-filter algorithm and the limiting-filter algorithm. The experimental test results of digital filtering are shown in Table 1.

According to the experimental test results, we take the experimental serial number as the abscissa and the discrete measurement value of the tension. The sampling value is the ordinate to draw the digital filtering algorithm test line chart. Fig. 6(a) is a line graph of the test results of a single median-filter algorithm. The blue curve represents the original sampled data, and the orange curve represents only the median-filtered data. Fig. 6(b) is a broken line graph of the test results of the median-filter algorithm and the limiting-filter algorithm. The blue curve represents the data after the median filter, and the orange curve represents the data after the limiting filter based on the median filter.

TABLE 1. Digital filter test result data.

Experiment number	Raw data	Median-filtered data	Fusion-filtered data
1	2300	2923	2923
2	2230	2923	2923
3	3396	2923	2923
4	2923	2923	2923
5	4187	2923	2923
6	2476	2476	2923
7	1672	2476	2923
8	4612	2476	2923
9	2305	2476	2923
10	2960	2476	2923
…	…	…	…
991	1038	2163	2983
992	4383	2163	2983
993	2163	2163	2983
994	1140	2163	2983
995	2672	2163	2983
996	1316	1603	2983
997	4210	1603	2983
998	1402	1603	2983
999	3916	1603	2983
1000	1603	1603	2983

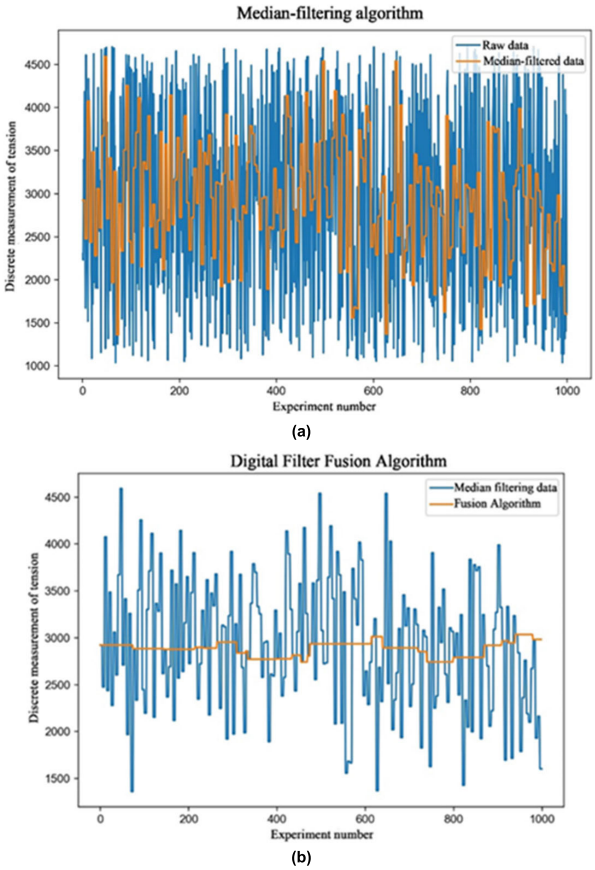

FIGURE 6. Line chart of the digital filtering algorithm's test results. (a) is a line chart of the single median filtering algorithm's test results; (b) is a line chart of the median filtering and limiting filtering algorithms' fusion test results.

It can be clearly seen from the test results that after a single median filtering algorithm, the fluctuation range of the

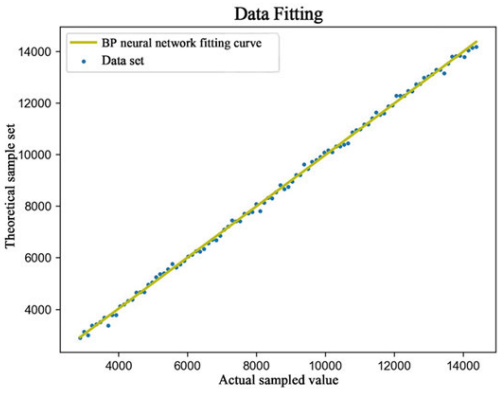

FIGURE 7. Fitting effect of the BP neural network algorithm.

tension signal sampling value is considerably reduced, but the sampling value is still in an unstable fluctuation state. The sampling value of the tension signal after the fusion of the median filter algorithm and the limit filter algorithm tends to be stable, and it is close to the theoretical value of 2875, concentrated at approximately 2750, and the average deviation is approximately 130. Compared with the total range, the error is 0.056%, and the effect is excellent.

In summary, the results of the experimental test verify that the digital filtering algorithm that combines the median filtering and the limiting filtering algorithms has a good filtering effect on mixed invalid interference data. This method can further improve the loom tension at the software level. We check the anti-interference ability of the system.

2) DATA FITTING EXPERIMENT

The BP neural network used in this paper is a three-layer structure with two inputs and one output. The two inputs are the actual sample value of tension and the ambient temperature data. The two input data and the theoretical tension value constitute the dataset. The BP neural network algorithm is used to fit and analyze 100 groups of tension data from 10 kg to 50 kg when the ambient temperature is 15 °C. The theoretical ideal sampling values corresponding to the response range are 2875 to 14375. The data training set composed of the theoretical sampling values and the actual sampling values is shown in Table 2.

The actual sampling value is taken as the horizontal coordinate, and the theoretical sampling value is used as the ordinate to draw the line graph. In Fig. 7, the fitting effect of the BP neural network algorithm is shown, and the curve fitted by the BP neural network algorithm has a nonlinear form. Using software to track the training effect or the fitting error and loss, the final fitting error reaches 0.0105%, and the fitting effect is excellent.

B. ON-SITE PRODUCTION ENVIRONMENT TEST OF THE LOOMS

On-site testing experiments are completed in the production workshop, and the ambient temperature is 10 °C. Fig. 8 shows the on-site inspection device of different angles after the loom

TABLE 2. BP neural network algorithm data fitting dataset.

Data serial number	Theoretical sampling value	Actual sampling value
1	*2875*	*2904*
2	*2991*	*3141*
3	*3107*	*3002*
4	*3223*	*3384*
5	*3339*	*3438*
6	*3455*	*3508*
7	*3572*	*3679*
8	*3688*	*3381*
9	*3804*	*3797*
10	*3920*	*3794*
11	*4037*	*4129*
12	*4153*	*4205*
13	*4269*	*4334*
14	*4385*	*4384*
15	*4501*	*4656*
16	*4617*	*4677*
17	*4734*	*4680*
18	*4850*	*4961*
19	*4966*	*5043*
20	*5082*	*5255*
21	*5198*	*5375*
...	...	...
92	*13446*	*13158*
93	*13562*	*13541*
94	*13678*	*13805*
95	*13794*	*13823*
96	*13910*	*13842*
97	*14027*	*13797*
98	*14143*	*14055*
99	*14259*	*14154*
100	*14375*	*14177*

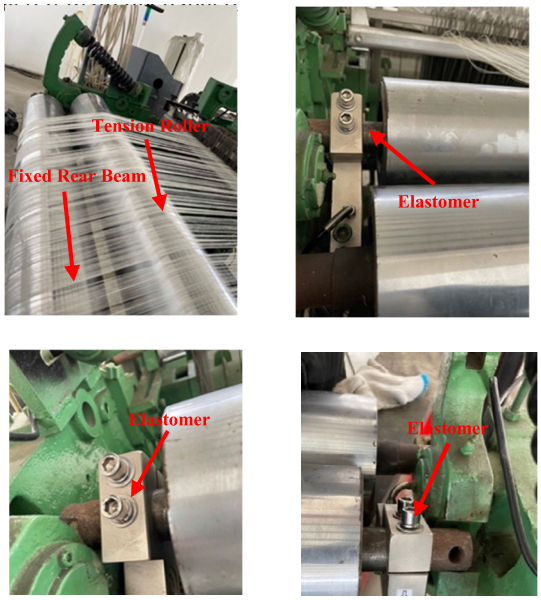

FIGURE 8. On-site experimental device of the tension detection system.

that has been laid with yarn is fixed on the back beam and the tension roller, while the elastic body is fixed on the loom.

To better explore the detection effect of the new system and its influence on the tension control effect of the loom,

TABLE 3. Test data of the original system and new system.

Data serial number	Original system detection value	New system detection value
1	*94.5 kg*	*96.1 kg*
2	*96.7 kg*	*95.8 kg*
3	*94.4 kg*	*96.2 kg*
4	*97.7 kg*	*95.8 kg*
5	*96.9 kg*	*95.5 kg*
6	*94.4 kg*	*96.0 kg*
7	*94.5 kg*	*95.5 kg*
8	*98.3 kg*	*95.4 kg*
9	*94.8 kg*	*96.0 kg*
10	*95.4 kg*	*96.3 kg*
...	...	...
191	*98.1 kg*	*95.5 kg*
192	*95.2 kg*	*96.5 kg*
193	*95.9 kg*	*95.5 kg*
194	*95.3 kg*	*95.9 kg*
195	*98.0 kg*	*95.7 kg*
196	*98.0 kg*	*96.5 kg*
197	*95.8 kg*	*96.3 kg*
198	*95.0 kg*	*96.8 kg*
199	*96.0 kg*	*95.3 kg*
200	*96.6 kg*	*95.8 kg*

except for the replacement of the detection system, the other structures of the loom and the tension control algorithm adopted remain unchanged.

The specific process of using the field device experiment is as follows:

(1) First, install the elastic body on the on-site loom, connect the various modules of the loom tension detection system, the system circuit board communicates with the computer through the serial port, and use the 24 V power supply to supply power to the detection system to ensure the accuracy of the detection data. In addition, reliability, the test system is powered on for a quarter of an hour before starting the experimental test.

(2) Open the serial port debugging assistant on the computer, read the tension value in real time, and complete the zero calibration of the detection system.

(3) The yarn tension of the loom was set to 96 kg, and the real-time tension value was recorded.

(4) We select 200 consecutive tension data for analysis and compare it with the tension detection value of the original tension detection system by drawing the tension curve graph.The continuous tension values of the new system and the original system are counted, and the following Table 3 is obtained.

The selected continuous tension value is compared and analyzed with the continuous tension value of the original detection system, as shown in Fig. 9.

As shown in Fig. 9, the blue curve represents the preset yarn tension of the loom, which is 96 kg, the orange curve represents the tension detection curve of the original system, and the green curve represents the tension detection curve of this system. The tension curve drawn by the value detected

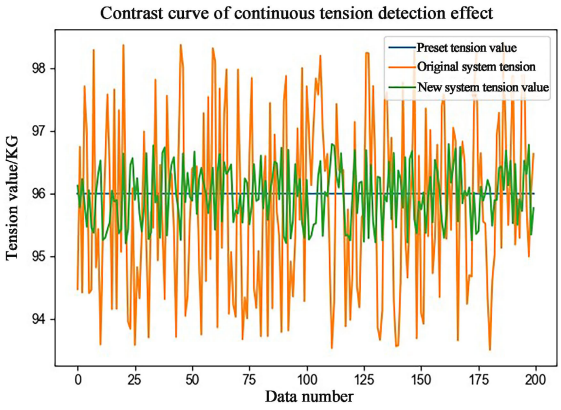

FIGURE 9. Comparison curve of the continuous tension detection effect.

by the original detection system has a large fluctuation, and the fluctuation range is approximately 3 kg, which means that the detection effect of the system is not stable enough, and there is a large error. The tension detection curve of the tension detection system proposed in this paper has a small fluctuation, the fluctuation range is approximately 0.8 kg, the error is small, and the detection accuracy is high.

The range of the original tension detection system is 500 kg. Through data analysis, it can be seen that the tension detection fluctuation range of the original detection system is approximately 2.5 kg, and the measured tension detection error is approximately 0.3%. The tension detection fluctuation range is 0.8 kg, and the measured tension detection error is 0.1%.

C. A COMPARATIVE ANALYSIS OF DATA FITTING ALGORITHMS

The least squares method is the most widely used data fitting algorithm and is typically used to address linear fitting problems. Therefore, in the traditional tension detection system, to apply the least squares method, some of the requirements for the tension detection effect are sacrificed. Usually, the influence of ambient temperature on the detection effect is ignored.

To reflect the actual situation, the environmental temperature factor is added for comparative analysis, and the tension data is collected under environments of 10°C, 15°C, 20°C, 25°C, 30°C, 35°C and 40°C. To reduce other factors and focus on the algorithm comparison, the tension value of 10 kg is selected as the analysis object. The statistical results of the data fitting errors are shown in Table 4.

Table 4 shows the sampled value for 10 kg of tension at a temperature of 10°C-40°C, as well as the fitting errors between the data fitting result of the least square method, the BP neural network algorithm and the ideal theoretical value. The fitting error of the least squares method fluctuated from 0.1% to 0.2%, while the fitting error of the BP neural network is reduced to 0.1% or less, showing the superiority of the BP neural network algorithm. The data shown in Table 4 is drawn into a line graph shown in Fig. 10.

TABLE 4. Data fitting error statistics at different temperatures.

Temperature	Theoretical sampling value	Least squares method		BP neural network method	
		fitted value	Fitting error	fitted value	Fitting error
10℃	*2875*	*2910.94*	0.125%	*2876.81*	0.063%
15℃	*2875*	*2902.03*	0.094%	*2873.36*	0.057%
20℃	*2875*	*2810.89*	0.223%	*2878.31*	0.115%
25℃	*2875*	*2925.31*	0.175%	*2872.90*	0.073%
30℃	*2875*	*2833.03*	0.146%	*2872.59*	0.084%
35℃	*2875*	*2916.69*	0.145%	*2877.21*	0.077%
40℃	*2875*	*2841.94*	0.115%	*2872.96*	0.071%

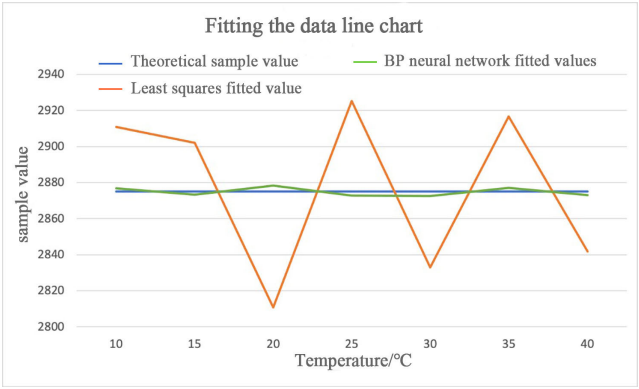

FIGURE 10. Line graph of data fitting value changes with temperature.

As shown in Fig. 10, the blue line represents the theoretical sampling value under 10 kg of tension, orange represents the fitting value of the least square method, and green represents the fitting value of the BP neural network. It can be seen from the figure that the sampling value obtained by BP neural network fitting fluctuates steadily. This is because the BP neural network integrates the environmental temperature factors, and the fitting is a nonlinear curve, whereas that of the least square method is linear, which deviates from the actual working state of tension detection.

D. RESULTS AND DISCUSSION

Through the experimental platform test in the laboratory environment, the field loom experimental platform test, and the data fitting algorithm comparison and analysis of the experimental simulation test, the effectiveness and rationality of the tension control strategy for the rapier loom proposed in this paper can be concluded, and the rapier loom tension control strategy can be improved, including the tension control precision of the rod loom. The testing process and the results of these experiments are based on the following assumptions and constraints:

(1) The range of the loom tension detection system designed in the experiment is 800 kg.

(2) In the process of the digital filtering algorithm fusion simulation experiment, the selected tension size is 10 kg, and the corresponding theoretical sampling value is 2875.

(3) In the process of the BP neural network algorithm data fitting experiment, the BP neural network architecture is composed of a three-layer structure design with two inputs and one output. The two inputs are the actual sampling value of the tension and the dataset composed of the environmental temperature data, as well as the theoretical tension value. The input matrix is expressed as $X=[X_1, X_2]$. The model needs to augment the input matrix X and then multiply it by the parameter θj ($0 \leq j \leq M$), which is equivalent to the neural network's bias term.

(4) In the on-site production environment test of the loom, the yarn tension of the loom is set to 96 kg.

(5) In the process of the BP neural network algorithm data fitting experiment, the ambient temperature is restricted to a slight fluctuation at approximately 15°C, and 100 sets of data in the tension sampling data of 10 kg to 50 kg are fitted and analyzed.

(6) In the data fitting comparison experiment with the least square method, to reduce the interference of other factors and focus on the comparison and analysis of the actual effect of the algorithm, a tension value of 10 kg is selected for the data analysis.

VI. CONCLUSION

This paper introduces the BP neural network algorithm and the digital filter algorithm to the tension control field of rapier looms. At the tension detection signal processing level, a new tension control strategy is proposed: a rapier loom tension control strategy based on the fusion of a BP neural network and a digital filter algorithm. A digital filtering algorithm fusion experiment, a BP neural network data fitting experiment and a fitting data algorithm comparative analysis experiment prove the superiority of the algorithm proposed in this paper, as well as the rationality and effectiveness of the method. This control strategy improves the precision of the tension control of rapier looms. It presents a new research perspective of high-precision and nonlinear processing of the tension detection signal, which extends the existing research on the optimization of the tension detection signal. The strategy enriches the research content of tension control strategies for rapier looms. The main conclusions drawn from the experimental results are as follows:

(1) The BP neural network algorithm after the optimization of the learning rate design is used to track the fitting error during the data fitting experiment. The final fitting error is 0.0105%, the fitting effect is excellent, and there is no "overfitting." The data demonstrates the rationality and superiority of the optimized BP neural network algorithm, which perfects the theoretical system of the BP neural network algorithm.

(2) The simulation test results after the limiting-filter algorithm and the median-filter algorithm have an error of 0.056% compared to the total range, and the effect is excellent. The results show that the fusion digital filter algorithm can reduce the fluctuation amplitude of the tension

detection signal, and an excellent sample dataset can be obtained.

(3) Through comparative experiments with the most commonly used fitting data algorithm, the least squares method, the fitting error of the least squares method is between 0.1% and 0.2%, whereas the fitting error of the BP neural network is within 0.1%, indicating the superiority of the optimized BP neural network algorithm.ss

(4) The tension control strategy for rapier looms proposed in this paper applies a combined digital filter algorithm and BP neural network algorithm to the information processing level of tension detection without changing the hardware structure or increasing the development costs. Effectively improving the tension control accuracy and manufacturing quality is of great practical importance for improving the production efficiency and fabric quality of rapier looms.

(5) The tension detection fluctuation range of the tension detection strategy proposed in this paper in the real machine experimental environment is 0.8 kg, and the measured tension detection error is 0.1%. The tension detection fluctuation range of the original detection system is approximately 2.5 kg, and the measured tension detection error is approximately 0.3%. Compared with the original detection system, the tension detection accuracy is greatly improved.

The tension control strategy for rapier looms presented in this paper is feasible and stable. Nevertheless, it also has shortcomings. In this paper, the algorithm comparison part of the experimental simulation test focuses on the algorithm comparison to reduce other factors, and only selects a sample tension. The numerical value is used as the analysis object, but in the actual let-off mechanism, the tension value changes due to different fabrics. Therefore, when changing the tension value, the control accuracy of the two algorithms are different. In future research, several actual working parameters can be extended to verify the effect of the algorithm's tension control from multiple angles.

This paper focuses on optimization of the BP neural network and its combination with digital filtering algorithms. In addition, there are some intelligent algorithms, such as genetic autodisturbance rejection control and model predictive control, that can be used for tension control of rapier looms. Therefore, according to the research content of this article, other algorithms can be studied in follow-up research to discover better tension control strategies for rapier looms.

REFERENCES

[1] C. Nagpal, P. K. Upadhyay, S. Shahzeb Hussain, A. C. Bimal, and S. Jain, "IIoT based smart factory 4.0 over the cloud," in *Proc. Int. Conf. Comput. Intell. Knowl. Economy (ICCIKE)*, Dubai, United Arab Emirates, Dec. 2019, pp. 668–673.

[2] Y. Jianjun and F. Youdong, "Application analysis of new automation intelligent technology in textile enterprises," *Heilongjiang Textile*, no. 2, pp. 23–25, 2020.

[3] G. Ramirez A., M. A. Valenzuela, S. Pittman, and R. D. Lorenz, "Modeling and evaluation of paper machine coater sections part 1: 1-Coater section and tension setpoints," *IEEE Trans. Ind. Appl.*, vol. 55, no. 2, pp. 2144–2154, Mar. 2019.

[4] W. Junqing, M. Peipei, G. Li, L. Baorong, and Z. Lele, "Analysis on the current situation and development trend of textile industry," *East, West, North, South*, no. 24, p. 130, 2019.

[5] W. Liu, X. Wu, X. Du, G. Xu, and S. Wang, "Tension networked control strategy for carbon fiber multilayer diagonal loom," *IEEE Access*, vol. 8, pp. 32280–32289, 2020.

[6] G. Xu, R. Zhou, W. Liu, and F. Hao, "The equivalent sliding mode tension control of carbon fiber multilayer diagonal loom," *Int. J. Control, Autom. Syst.*, vol. 17, no. 7, pp. 1762–1769, Jul. 2019.

[7] Y. Lin, G. R. Liu, and G. Wang, "A particle-based free surface detection method and its application to the surface tension effects simulation in smoothed particle hydrodynamics (SPH)," *J. Comput. Phys.*, vol. 383, pp. 196–206, Apr. 2019.

[8] W. Liu, S. Wang, F. Shi, G. Xu, and Y. Cheng, "Application of adaptive control on carbon fiber diagonal loom," *Int. J. Control, Autom. Syst.*, vol. 19, no. 3, pp. 1283–1290, Mar. 2021.

[9] W. Liu *et al.*, "Tension networked control strategy for carbon fiber multilayer diagonal loom," *IEEE Access*, 2020.

[10] A. Karnoub, N. Kadi, and Z. Azari, "Using the expert system to analyze loom performance," *J. Textile Inst.*, vol. 108, pp. 1–13, May 2016.

[11] Q. Xu, S. Q. Mei, and Z. M. Zhang, "Measurement method of yarn tension based on CCD technology," *Adv. Mater. Res.*, vols. 230–232, pp. 89–93, 2011.

[12] H. Banitalebi and M. Rafeeyan, "A new approach for non contact measuring of tension in fixed and moving wires," *Int. J. Adv. Design Manuf. Technol.*, vol. 5, no. 4, pp. 51–57, 2013.

[13] Y. Kikuchi and T. Ishihara, "Anomaly detection and prediction of high-tension bolts by using strain of tower shell," *Wind Energy*, no. 2, pp. 1–16, 2020.

[14] M. L. C. Passos and M. L. M. F. S. Saraiva, "Detection in UV-visible spectrophotometry: Detectors, detection systems, and detection strategies," *Measurement*, vol. 135, pp. 896–904, Mar. 2019.

[15] L. Xu, N. Shoaie, F. Jahanpeyma, J. Zhao, M. Azimzadeh, and K. T. Al-Jamal, "Optical, electrochemical and electrical (nano)biosensors for detection of exosomes: A comprehensive overview," *Biosensors Bioelectron.*, vol. 161, Aug. 2020, Art. no. 112222.

[16] A. Kim, C. Lee, and J. Kim, "Durable, scalable, and tunable omniphobicity on stainless steel mesh for separation of low surface tension liquid mixtures," *Surf. Coatings Technol.*, vol. 344, pp. 394–401, Jun. 2018.

[17] J. Cao, K. Udhayakumar, R. Rakkiyappan, X. Li, and J. Lu, "A comprehensive review of continuous-/discontinuous-time fractional-order multidimensional neural networks," *IEEE Trans. Neural Netw. Learn. Syst.*, early access, Dec. 28, 2021, doi: 10.1109/TNNLS.2021.3129829.

[18] D.-X. Zhou, "Universality of deep convolutional neural networks," *Appl. Comput. Harmon. Anal.*, vol. 48, no. 2, pp. 787–794, Mar. 2020.

[19] O. Yılmaz, E. Bas, and E. Egrioglu, "The training of pi-sigma artificial neural networks with differential evolution algorithm for forecasting," *Comput. Econ.*, vol. 272, pp. 1–13, Mar. 2021.

[20] A. N. Yildirim, E. Bas, and E. Egrioglu, "Threshold single multiplicative neuron artificial neural networks for non-linear time series forecasting," *J. Appl. Statist.*, vol. 48, nos. 13–15, pp. 2809–2825, Nov. 2021.

[21] Y. C. Lin, Y.-J. Liang, M.-S. Chen, and X.-M. Chen, "A comparative study on phenomenon and deep belief network models for hot deformation behavior of an Al–Zn–Mg–Cu alloy," *Appl. Phys. A, Solids Surf.*, vol. 123, no. 1, p. 68, Jan. 2017.

[22] Y. C. Lin, J. Li, M.-S. Chen, Y.-X. Liu, and Y.-J. Liang, "A deep belief network to predict the hot deformation behavior of a ni-based superalloy," *Neural Comput. Appl.*, vol. 29, no. 11, pp. 1015–1023, Jun. 2018.

[23] H. Huang, J. Xu, K. Sun, L. Deng, and C. Huang, "Design and analysis of tension control system for transformer insulation layer winding," *IEEE Access*, vol. 8, pp. 95068–95081, 2020.

[24] F. Meng, S. Liu, and K. Liu, "Design of an optimal fractional order PID for constant tension control system," *IEEE Access*, vol. 8, pp. 58933–58939, 2020.

[25] E. Al-Rawachy, R. P. Giddings, and J. Tang, "Experimental demonstration of a real-time digital filter multiple access PON with low complexity DSP-based interference cancellation," *J. Lightw. Technol.*, vol. 37, no. 17, pp. 4315–4329, Sep. 1, 2019.

[26] F. Yan, K. Fan, X. Yan, and S. Li, "Constant tension control of hybrid active-passive heave compensator based on adaptive integral sliding mode method," *IEEE Access*, vol. 8, pp. 103782–103791, 2020.

[27] V. S. Borges, E. G. Nepomuceno, C. A. Duque, and D. N. Butusov, "Some remarks about entropy of digital filtered signals," *Entropy*, vol. 22, no. 3, p. 365, Mar. 2020.

[28] P. Lyakhov, M. Valueva, G. Valuev, and N. Nagornov, "A method of increasing digital filter performance based on truncated multiply-accumulate units," *Appl. Sci.*, vol. 10, no. 24, p. 9052, Dec. 2020.
[29] A. Sankoh, W. Jin, Z. Zhong, J. He, Y. Hong, R. P. Giddings, I. Pierce, M. O'Sullivan, J. Lee, T. Durrant, and J. Tang, "Hybrid OFDM-digital filter multiple access PONs utilizing spectrally overlapped digital orthogonal filtering," *IEEE Photon. J.*, vol. 12, no. 5, pp. 1–11, Oct. 2020.
[30] H. Park, M. Yu, Y. Jung, and S. Lee, "Design of reconfigurable digital if filter with low complexity," *IEEE Trans. Circuits Syst. II, Exp. Briefs*, vol. 66, no. 2, pp. 217–221, Feb. 2019.
[31] Z. Luo, C. Liu, and S. Liu, "A novel fault prediction method of wind turbine gearbox based on pair-copula construction and BP neural network," *IEEE Access*, vol. 8, pp. 91924–91939, 2020.
[32] X. Tian, L. Kong, D. Kong, L. Yuan, and D. Kong, "An improved method for NURBS surface based on particle swarm optimization BP neural network," *IEEE Access*, vol. 8, pp. 184656–184663, 2020.
[33] J. Lee, J. Byeon, and C. Lee, "Theories and control technologies for web handling in the Roll-to-Roll manufacturing process," *Int. J. Precis. Eng. Manufacturing-Green Technol.*, vol. 7, no. 2, pp. 525–544, Mar. 2020.
[34] D. Magura, K. Kyslan, S. Padmanaban, and V. Fedák, "Distribution of the strip tensions with slip control in strip processing lines," *Energies*, vol. 12, no. 15, p. 3010, Aug. 2019.
[35] T. Longfei, X. Zhihong, and B. Venkatesh, "Contactor modeling technology based on an artificial neural network," *IEEE Trans. Magn.*, vol. 54, no. 2, pp. 1–8, Feb. 2018.

YANJUN XIAO received the bachelor's degree in industrial automation chemistry and the master's degree in machine manufacturing and automation from the Hebei University of Technology. He currently works as a Professor at the School of Mechanical Engineering, Hebei University of Technology. His main research interests include waste heat recovery and industrial control.

FURONG HAN graduated from the Hebei University of Technology, in 2020. She is currently pursuing the master's degree with the Hebei University of Technology. Her research interests include intelligent control and health management.

WEILING LIU received the Ph.D. degree from Tianjin University, in 2006. She is currently an Associate Professor. She teaches measurement and control technology with the Instrument Department, Hebei University of Technology. Her research interests include new perception and control systems.

FENG WAN currently works as an Associate Professor at the School of Mechanical Engineering, Hebei University of Technology. His main research interests include application research and instrument development of spectral technology.

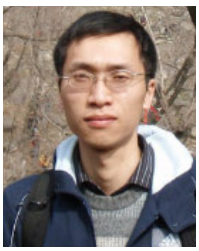

KAI PENG received the Ph.D. degree. He currently works with the School of Mechanical Engineering, Hebei University of Technology. His research interests include geometric measurement technology, machine vision, and application.